Supplemental Data

A Simple Vision-Based Algorithm for Decision Making in Flying *Drosophila*

Gaby Maimon, Andrew D. Straw, and Michael H. Dickinson

Supplemental Discussion

Role of Nondirectional Mechanisms in Explaining the Free-Flight Distributions

During flight, behavioral reactions to the long and short post can be either directional (i.e., taxis) or nondirectional (i.e., kineses). A directional mechanism would involve explicitly steering toward or away from the objects. A nondirectional mechanism would involve a change in translational speed or the rate of turning as a function of distance to the objects. The role of directional mechanisms in explaining the free-flight distributions is discussed in the main text (Figure 2).

To examine the role of non-directional mechanisms, we plotted translational speed and angular velocity in the tunnel (Figures S2A–S2C) and found that the flies did in fact slow down and turn more when they were within 3 cm of the long post—a velocity pattern that may have contributed to the increased residence probability near the long object. A decrease in translational speed is expected in this region because as the post loomed, many animals exhibited a collision-avoidance saccade, a stereotyped behavior that involves a transient decrease in flight speed [S1]. However, the attractiveness of the long post was manifest at distances greater than 3 cm, indicating that a spatial modulation of flight velocity was not the only factor at play. The velocities of the flies in the presence of the short post did not differ substantially from those in the no-post condition, except for a weak increase in angular velocity (i.e., increased turning) 0–5 cm from the small object.

One can further assess the influence of flight speed by plotting probability histograms in which bin values are incremented when a fly first enters each tiny region, but not for subsequent consecutive samples within the region. In these "flux" transit-probability histograms, slow- and fast-moving flies contribute equally to the final distribution. We performed this normalization, which removed ~90% of the original sample points (samples removed: 381728/426879 with the long post, 281353/314232 with the short post, 281353/314232 with no post). The resulting distributions resembled the unnormalized plots (Figures S2D and S2E), indicating that changes in flight speed do not explain the major differences in the residence probability across conditions.

Explanation of 1 Hz Behavioral Oscillation to Small Stripes Presented in Open-Loop Directly in Front of the Flies

Small bars directly in front of the flies drove a 1 Hz oscillation in the steering response (Figure 4B, middle row, right two columns). These short-stripe oscillations were smaller in amplitude and slightly phase advanced (~45°) to those driven by a long stripe; however, they probably still reflected an attractive response because they were not 180° out of phase and aversion did not typically show fast dynamics. These responses to small stripes oscillating directly in front of the animal suggest that many of our stimuli probably engaged both the attractive and repulsive pathways simultaneously, albeit with a relative strength that depended on stripe length. In this view, the motor programs for attraction and repulsion are not mutually exclusive and the net behavior of the flies represents a summation of two parallel pathways, not a "winner-take-all" scheme [S2, S3].

Supplemental Experimental Procedures

Flies

We studied 3- to 5-day-old *Drosophila melanogaster* Miegen from our laboratory stock. Flies were anaesthetized on a Peltier stage held at ~4°C, and females were selected for experimentation. The animals were given at least 30 min to recover from anesthesia.

Free Flight

We placed flies in an enclosed tunnel (31 × 31 × 86 cm) and tracked their 3D flight trajectories, which were reconstructed from five simultaneously captured 2D video images taken through the tunnel's clear plexiglass ceiling (see below). The arena was illuminated from above with infrared LEDs at a wavelength to which the animals are blind (880 nm). The arena had a black floor and white side walls. Green LEDs were used to back-project an array of circles (~6 cm diameter) on the two long side walls of the tunnel. These background patterns provided contrast to help the animals orient. In each experiment, ten sated flies were placed in the arena for at least 12 hr. The system could track up to two flies simultaneously, and it was rare that more than two flies flew at once. During each 12 hr run, we recorded roughly 300 trajectories that were >3 s long, or ~30 trajectories for each individual. However, we could not uniquely identify individual flies, and thus our data set contains pseudoreplication. We conducted three experiments with the long post, three experiments with the short post, and four experiments with no post. Data across different experiments were consistent and therefore combined for analysis. In post analysis, trajectories were purposefully clipped 2 cm away from the arena's walls, floor, and ceiling so as to remove bouts of walking from the data set.

Free-Flight Tracking System

We used five monochrome digital cameras that captured images at 100 frames per s (model A602f, Basler Vision Technologies, Germany). Each camera was connected via IEEE 1394 bus to a dedicated image processing computer, which extracted the 2D position of the fly's image by means of a background subtraction algorithm. These coordinates were transmitted over gigabit ethernet LAN to a central computer, which performed the 2D-to-3D triangulation and tracking. The basic algorithm was a linear least-squares fit of the intersection of N rays, defined by the 2D image points and 3D camera centers of each of the N cameras [S4]. Only processed data were saved, although some raw image sequences were also stored for verification purposes. The mean re-projection error from the 3D coordinates versus the original 2D image-space coordinates was less than 0.5 pixels.

With a simple dynamic model and Bayesian statistics in the form of a Kalman filter, an online prediction was made of the 3D position, velocity, acceleration, and associated covariance matrix of the fly in the current and subsequent frames. The model, which was linear and discrete, was an update matrix describing the laws of motion for a particle in which maneuvering is performed through changes in acceleration. The prediction from the prior frame was used in following frames so that we could determine which 2D features, and which cameras, were most likely to contain useful information about the position of the tracked fly. Trajectories ended when the fly had not been observed for several frames.

Camera calibrations were obtained in two ways. First, we used a relatively high-error calibration to estimate the camera centers with images of calibration objects and the Direct Linear Transformation (DLT) algorithm [S5]. Although this calibration can be used for tracking, it does not, in the form we used, deal with optical distortions related to deviations from a pinhole camera and it uses only a few, manually entered, 3D points and 2D image locations. Therefore, we also used an automated "Multi-Camera Self Calibration" algorithm and software [S6]. This method constrains the camera locations by utilizing the inherent redundancy when three or more cameras view a single 3D point. By recording raw 2D coordinates of fly positions as

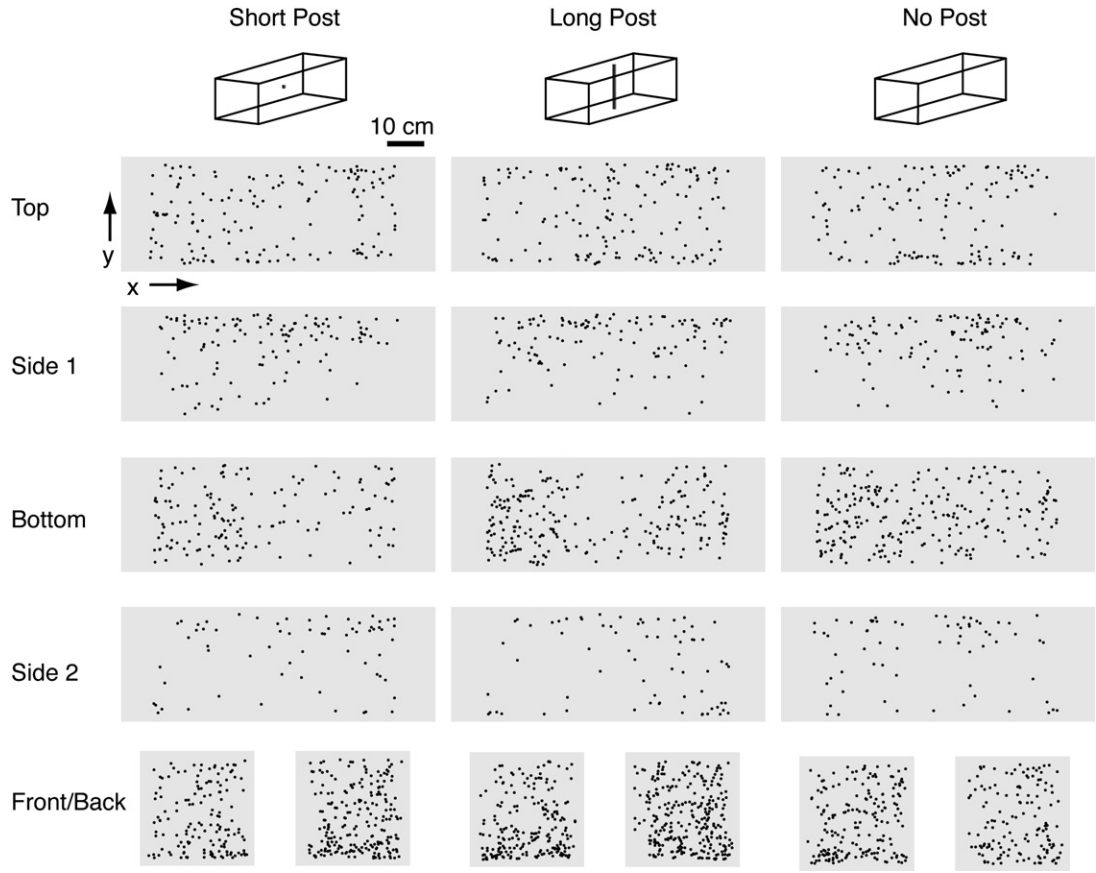

Figure S1. Trajectory Start Locations Do Not Differ Appreciably between Free-Flight Conditions

We extracted the start location of trajectories within the imaged volume (2 cm inward from the top, bottom, and two side walls; ~10 cm inward from the front and back walls) and plotted this coordinate as a point on the nearest surface edge. For analysis, trajectories had to start within 4 cm of the top, bottom, and two side walls and within ~12 cm of the front and back walls.

viewed by the individual cameras, for hundreds of different (unknown) 3D locations, a single, overdetermined solution is made. The camera centers from the DLT calibration are used to place this solution in lab frame coordinates. As a final step, the software iteratively estimated a nonlinear radial distortion term for each camera [6].

Tethered Flight

We attached a stainless-steel pin (127 μm diameter) to the fly's anterior notum by using ultraviolet-activated cement (Duro, Düsseldorf, Germany). The tether was attached such that the flies were in a normal hovering flight posture during experiments, with a pitch angle of ~60° from horizontal (Figure 3A). For some flies, we immobilized the head by gluing it to the tether; with other flies, we did not restrain the head (see below).

Flies were centered in a flight arena consisting of a cylindrical array of LEDs (Figure 3A). The complete display consisted of 32 rows × 96 columns of LEDs at a 7 cm radius surrounding the fly (94° high; 360° around). Eight columns of LEDs (~30°) were removed from the arena's rear to allow for inserting the tethered animal. This open area resided within the blind spot in the animal's rear visual hemifield. The luminance of the fully lit arena was 72 cd/m^2 [S7].

To measure steering responses, flies were illuminated with an infrared diode from above so that the flapping wings cast oscillating shadows over infrared sensors below, with one sensor per wing. The sensors yielded oscillating signals whose amplitude and frequency provided a measure of wing-stroke amplitude and frequency with time [S8]. The difference in bilateral stroke amplitude is highly correlated with yaw torque [S9], thus indicating an intended turn. All tethered-flight data were sampled at 1 kHz.

In closed-loop experiments, the difference between the left and right wingbeat amplitude was fed back to control the angular velocity of the visual pattern, a 15°-wide vertical stripe. Stripe height varied pseudorandomly across trials, ranging from 8° to 94°. We averaged 7.1 presentations of each stripe per animal, 20 s per presentation. This yielded ~2 min of closed-loop data per stripe (min 40 s; max 160 s). Between stimuli, we always showed the flies a full-length (94°-high) stripe for 8 s. Because the animals stabilized long stripes in the front visual field, this tended to standardize the behavioral state and stimulus position prior to each trial. The long-stripe intertrial data are shown in the gray windows of Figure 3B and the left-most column of Figure 3D.

To create the polar plots in Figure 3, we ran a 2 s boxcar filter through the data at 200 ms steps. At each filter location, we treated the 2000 associated angular stripe positions as unit vectors and calculated their mean. The angle of this mean vector denoted the average stripe position within the window. The eccentricity (r) of the mean vector provided a measure of dispersion ($r \approx 1$ indicates low dispersion; $r \approx 0$ indicates high dispersion). We discarded the first two seconds of data for each stimulus to reduce any residual effects of the response to the stripe presented between trials. The polar plots allowed us to classify the behavior into three categories. Points with $r > 0.6$ and angles in the front hemifield denoted "fixation" (stripe was kept stably in the front). Points with $r > 0.6$ and angles in the rear hemifield denoted "antifixation" (stripe was kept stably in the back). Points with $r < 0.6$ denoted "spinning" (instability). Closed-loop data are shown only for head-glued flies. Head-free flies predominantly spun, rather than antifixated, the small stimuli, probably due to stimulus jitter associated with unmeasured head movements.

In the primary open-loop experiment (Figure 4), we presented flies with an oscillating 15°-wide vertical stripe of varying heights (8°–94°) and measured steering responses. Between stimulus presentations, we allowed the flies to fixate a long stripe in closed loop for 10 s. This returned the animals to a zero-mean turn response prior to the next trial. Stimuli were presented in a pseudorandom order for at least 10 s per presentation. Each stimulus

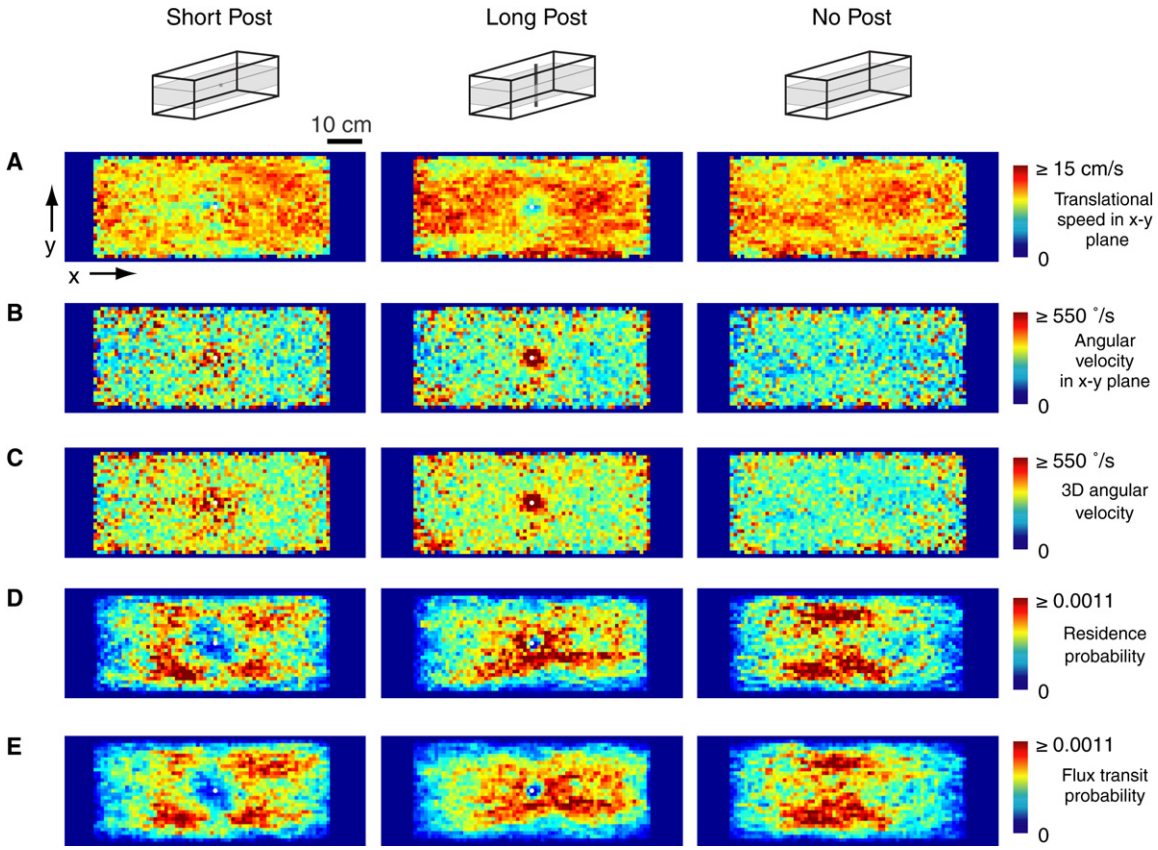

Figure S2. Nondirectional Changes in Free-Flight Velocities Do Not Fully Explain the Free-Flight Aggregations

(A) Mean translational speed, calculated using the central difference method and after collapsing all data to the x-y plane.
(B) Mean absolute value of angular velocity, calculated after collapsing all data to the x-y plane.
(C) Mean 3D angular velocity, calculated with the dot product between adjacent 3D heading vectors.
(D) Residence probability.
(E) Flux transit probability, in which histogram bin counters were only incremented when a trajectory first entered an x-y bin, but not for subsequent samples in the bin, thus normalizing for differences in flight speed. All plots in this figure show data from a 15-cm-thick middle z slice for better comparison of the long- and short-post data. White dots indicate the location of the posts, to scale.

was repeated one to four times per animal (mean 2.4). In a second open-loop experiment (Figure S5), we rotated either a 94°-high or 8°-high stripe (15° wide) around the animals at varying speeds, clockwise or counterclockwise. Between stimulus presentations, we allowed the flies to fixate a long stripe in closed loop for 10 s. Stimuli were presented for 2 s, or one full rotation cycle, whichever was longer for a given rotation speed. Each stimulus was presented in pseudorandom order, one to five times per animal (mean 3.8). In open-loop analyses, we pooled data from head-glued and head-free flies because these groups provided qualitatively similar results.

Supplemental References

S1. Tammero, L.F., and Dickinson, M.H. (2002). Collision-avoidance and landing responses are mediated by separate pathways in the fruit fly, Drosophila melanogaster. J. Exp. Biol. *205*, 2785–2798.

S2. Frye, M.A., and Dickinson, M.H. (2004). Motor output reflects the linear superposition of visual and olfactory inputs in Drosophila. J. Exp. Biol. *207*, 123–131.

S3. Sherman, A., and Dickinson, M.H. (2004). Summation of visual and mechanosensory feedback in Drosophila flight control. J. Exp. Biol. *207*, 133–142.

S4. Hartley, R.I., and Zisserman, A. (2000). Multiple view geometry in computer vision (Cambridge, U.K.: Cambridge University Press).

S5. Abdel-AzizY.I.KararaH.M.1971). Direct linear transformation from comparator coordinates into object space coordinates. American Society of Photogrammetry Symposium on Close-Range Photogrammetry, American Society of Photogrammetry, Falls Church, Virginia, 1–18.

S6. Svoboda, T., Martinec, D., and Pajdla, T. (2005). A convenient multicamera self-calibration for virtual environments. PRESENCE: Teleoperators and Virtual Environments *14*, 407–422.

S7. Reiser, M.B., and Dickinson, M.H. (2008). A modular display system for insect behavioral neuroscience. J. Neurosci. Methods *167*, 127–139.

S8. Götz, K.G. (1987). Course-control, metabolism and wing interference during ultralong tethered flight in *Drosophila melanogaster*. J. Exp. Biol. *128*, 35–46.

S9. Tammero, L.F., Frye, M.A., and Dickinson, M.H. (2004). Spatial organization of visuomotor reflexes in Drosophila. J. Exp. Biol. *207*, 113–122.

S10. Heisenberg, M., and Wolf, R. (1984). Vision in *Drosophila*: Genetics of Microbehavior (Berlin: Springer Verlag).

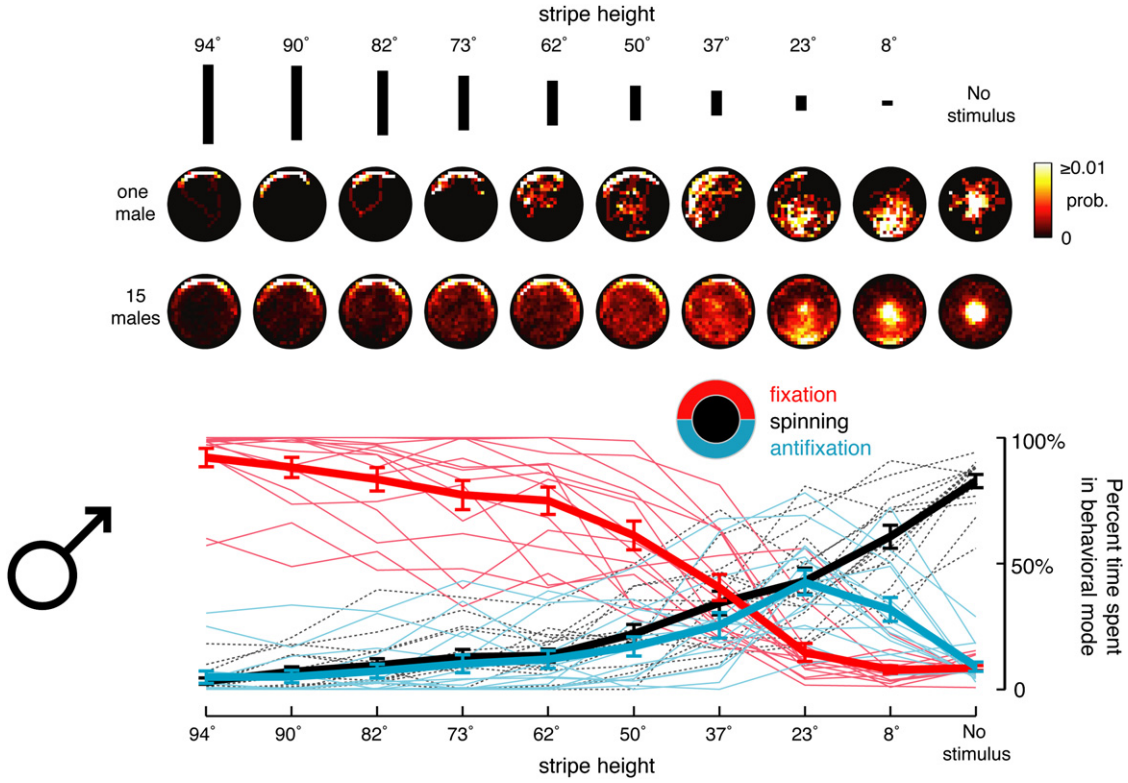

Figure S3. Male *Drosophila* Are Attracted to Long Stripes and Repelled by Short Stripes in Closed-Loop Tethered Flight

Data plotted in the same format as Figure 3D.

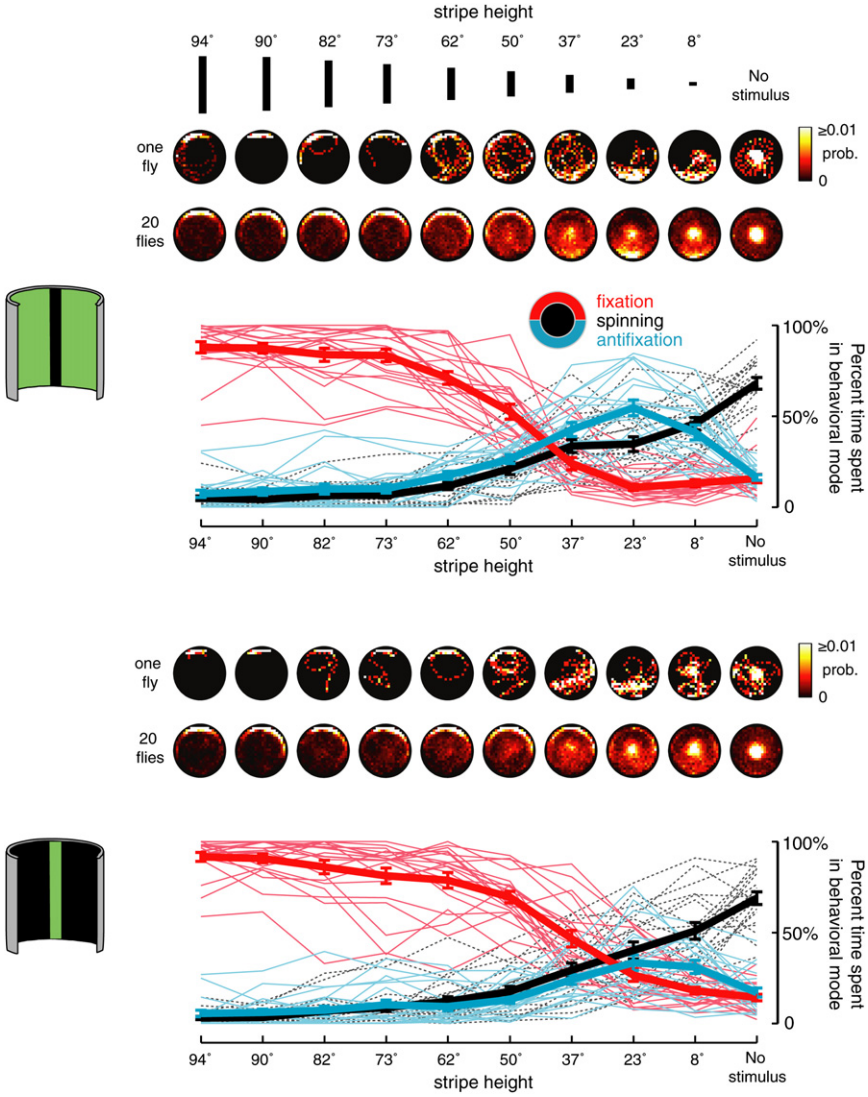

Figure S4. Flies Are Attracted to Long Stripes and Repelled by Short Stripes Independent of the Contrast Sign of the Stimulus

Closed-loop tethered-flight data plotted in the same format as Figure 3D. For each fly, we alternated between blocks of dark stripes, our typical stimulus, and bright stripes. Thus, the same 20 flies contributed data to each plot. For data presented in other figures, tethered-flight experiments were conducted in a dark room. However, when the bright stripe was the only source of luminance, we were concerned that its diffuse reflection might interfere with normal fixation behavior. For this reason, we turned on the overhead halogen lights during these experiments (for both dark and bright stripes) to reduce the contrast of the reflection. With halogen lights on, the Michelson contrast [(Imax − Imin)/(Imax + Imin)] was 0.883 for the bright stripe and 0.716 for the dark stripe (luminances of the stripe and a patch of LEDs immediately adjacent to the stripe were measured with a Minolta Chromameter CS-100A). In a dark room, contrast values were 0.996 for the bright stripe and 0.812 for the dark stripe. A prior brief report (Figure 109 in [S10]) suggested that *Drosophila* are innately attracted toward long dark stripes but are repelled by, or show ambiguous behavior in response to, long bright stripes. In our experiments, however, flies responded similarly to dark and bright stripes. There are several possible explanations for this discrepancy, including differences in closed-loop feedback gain, closed-loop apparatus (torque meter versus optical wingbeat analyzer), visual presentation (LED array versus backlit drum), genetic background of flies tested, and rearing conditions.

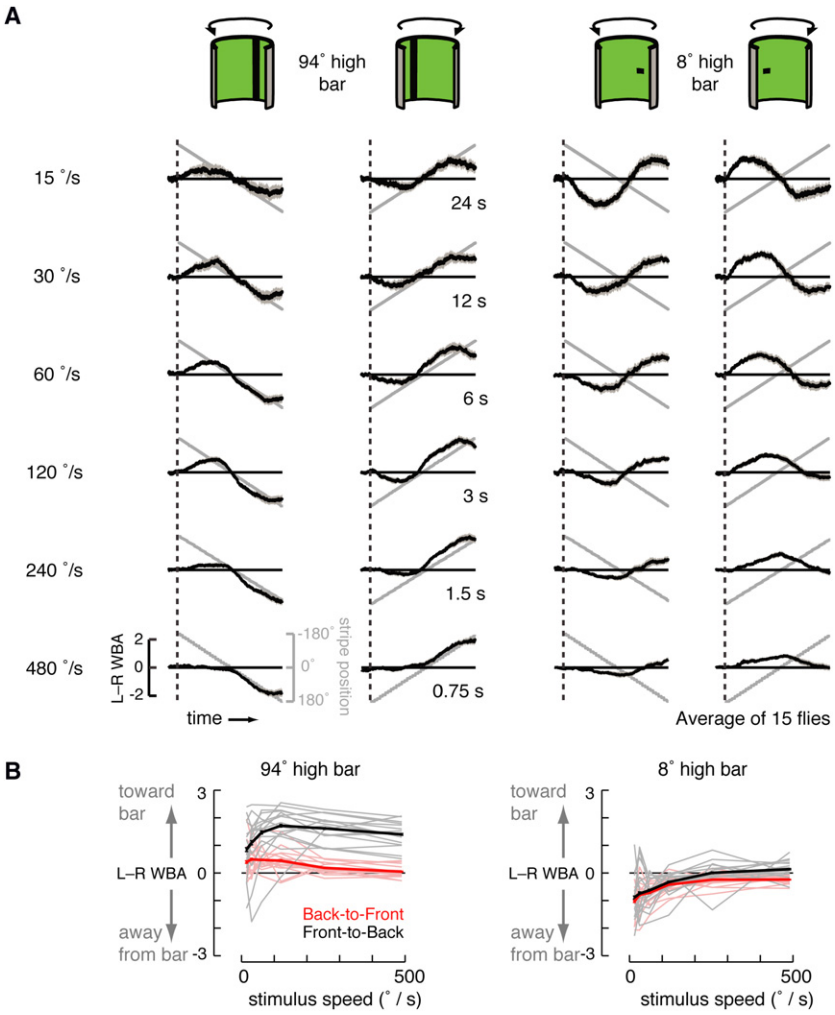

Figure S5. Long-Stripe Attraction and Short-Stripe Repulsion Differ in Sensitivity to Stimulus Speed and Direction

(A) Averaged turn responses of 15 flies to a 94°-high or an 8°-high stripe rotated around the arena in open-loop. Positive L-R WBA indicates turns to the right. Positive stimulus positions indicate bar locations on the left, and vice versa (note, however, that the stimulus position's y axis has been flipped, with positive values downward, so that turns toward the stimulus bring the steering-response and stripe-position curves closer together). 0° indicates the bar was directly in front of the flies. Standard errors are shown as gray regions around each curve.

(B) Mean responses are plotted as a function of stimulus speed. Responses from the first 40% of the rotation cycle—during back-to-front motion—are plotted in light red for individual flies and in dark red for the average (±SEM). Responses from the final 40% of the rotation cycle—during front-to-back motion—are plotted in gray for individual flies and in black for the average (±SEM). Clockwise and counterclockwise stimulus presentations were combined, and L-R WBA responses were inverted, as necessary, so that positive values indicate turning toward the stripe and negative values indicate turning away from the stripe.